

## Strain measurement of fiber optic sensor surface bonding on host material

Shiuh-Chuan HER, Chang-Yu TSAI

Department of Mechanical Engineering, Yuan Ze University, 135 Yuan-Tung Road, Chung-Li, Taiwan, China

Received 2 March 2009; accepted 30 May 2009

**Abstract:** Fiber optic sensor has been widely used as a structural health monitoring device by either embedding into or surface bonding onto the structures. The strain of optic fiber induced by the host material is strongly dependent on the bonding characteristics which include the protective coating, adhesive layer and the length of bonding. The strains between the fiber optics and host structure are not exact the same. The existence of the protective coating and adhesive layer would affect the strain measured by the surface bonding optic sensor. The analytical expression of the strain in the optic fiber induced by the host material was presented. The results were validated by the finite element method. The theoretical predictions reveal that the strain in the optical fiber is lower than the strain of host material. Parametric study shows that a long bonding length and high modulus of protective coating would increase the percentage of strain transferring into the optical fiber. Experiments were conducted by using Mach-Zehnder interferometer to measure the strain of the surface bonding optic fiber induced by the host structure. Good agreements were observed in comparison with the experimental results and theoretical predictions.

**Key words:** fiber-optic strain sensor; Mach-Zehnder interferometer; bonded length

### 1 Introduction

Fiber optical strain sensors possess several advantages over conventional electrical sensors such as light mass, small dimension, high temperature endurance, dielectric nature, and immunity to electromagnetic interference, which meet the basic requirements to be a smart structure sensing element. The revolutions in the fiber optic technology have enabled the development of fiber optic sensors. This development, in combination with advances in composite material, has opened up the new field of fiber optic smart structures which have the ability to sense environmental changes within or around the structure and are able to interpret and react to these changes. The direct application of smart structure in structural health monitoring is under intensive study over the last few years, particularly, in aerospace industry[1] and civil engineering[2]. Several fiber optic technologies have been proposed for strain/temperature measurements, such as fiber bragg grating (FBG) sensors[3–5], Fabry-Perot fiber optic sensors[6–7]. Optical fiber sensors based on fiber bragg grating have been demonstrated

successively in monitoring structures. LO[8] used FBG sensors to measure the axial strain and temperature simultaneously. CHAU et al[9] experimentally demonstrated the effectiveness of using FBG system for structural vibration control. Interferometric type fiber optic sensors have advantages of high sensitivity and potentially high spatial resolution. Therefore, they can be used for the damage detection in structural members [10–13]. As a sensor, it is expected that the strains between the optical fiber and host structure are the same. However, due to the existence of the adhesive layer and protecting coating, part of the energy would convert into the shear deformation. Thus, the strain of the optical fiber is different from the host structure. LAU et al[14] developed a simple model to calculate the percentage of strain applied to the host structure actually transferred to the embedded fiber optic sensor. In this investigation, the fiber optic sensor is surface bonded on the host structure. The relationship of strains between the host structure and surface bonded fiber optics is presented. The experimental tests based on the Mach-Zehnder interferometer are performed to measure the strain in the surface bonded optical fiber and compared with the theoretical prediction.

## 2 Strain in optic fiber

When the optical fiber is used as a sensor to monitor the strain or stress in a structure, the capability of measurement depends on the bonding characteristics between the optical fiber and host structure. The measuring sensitivity of the fiber optic sensor is affected by the protective coating, adhesive layer and bonding length. In this investigation, the optical fiber is surface bonded on the host structure while the external load stress or strain is applied on the host structure only. In fact, the deformation of optical fiber induced by the host structure is transferred via the adhesive layer and protective coating. The deformation of optical fiber induces the change of optical signal transmission. Since the stress or strain is directly applied to the host structure other than the optical fiber, so that the strain or stress in the optical fiber is subjected to shearing at the interface between the fiber and coating. The analytical model is shown in Fig.1 with cylindrical optical fiber and coating on the top and the host material under the bottom, adhesive in between. The host material is subjected to far field strain  $\epsilon_0$ . HER and TSAI [15] has derived the strain of optic fiber, based on the assumptions of perfectly bonding along the interfaces and shear deformation only in the coating and adhesive, as follows:

$$\epsilon_f = \frac{\epsilon_0}{E_f \left( \frac{\pi r_f^2}{2hr_p E_h} + \frac{1}{E_f} \right)} \left[ 1 - \frac{\cosh(\lambda_1 x)}{\cosh(\lambda_1 L_f)} \right] \quad (1)$$

$$\lambda_1 = \sqrt{\frac{2r_p \left( \frac{\pi r_f^2}{2hr_p E_h} + \frac{1}{E_f} \right) \int_0^{\cos^{-1}\left(\frac{b}{r_p}\right)} \left( \frac{r_p(1-\sin\theta)}{G_a} + \frac{r_p}{G_p} \ln\left(\frac{r_p}{r_f}\right) \right)^{-1} d\theta}$$

where  $E_h$  and  $E_f$  are the elastic moduli of the host material and optical fiber, respectively;  $G_a$  and  $G_p$  are the shear moduli of adhesive and coating, respectively;  $r_f$  and  $r_p$

are the radii of the optical fiber and coating, respectively;  $h$  is the thickness of the host material;  $b=0.2r_p$ ;  $L_f$  is half of the surface bonded length.

## 3 Parametric study

In this section, the parametric analysis was conducted by using Eq.(1) to investigate the influences of the bonded length, adhesive and coating on the optical fiber strain. The material properties for host material, adhesive, coating and optical fiber used in the numerical study are listed in Table 1. The outer radii of optical fiber and coating are  $r_f=62.5 \mu\text{m}$  and  $r_p=125 \mu\text{m}$ , respectively; the thickness of the host material  $h=8 \text{ mm}$ . The coefficient of refraction and pockel's constants are  $n_0=1.45$ ,  $p_{11}=0.17$ ,  $p_{12}=0.36$ , respectively. Prior to the parametric analysis, the theoretical prediction Eq.(1) of the strain in the optical fiber was validated by the finite element method using the commercial software ANSYS. Eight node elements (solid 45) were used to generate meshes as shown in Fig.2. The strain of the optical fiber along the surface bonded length calculated by Eq.(1) and finite element method are plotted in Fig.3. The optical fiber strain ( $\epsilon_f$ ) shown in Fig.3 is normalized by the far field strain ( $\epsilon_h$ ) which is applied to the host material. It is shown that the theoretical predictions are in good agreement with the FEM results. The distribution of the optical fiber strain shows that the maximum strain occurs in the middle of the surface bonded optic fiber and decreases to zero at both ends of the bonded length.

**Table 1** Material properties used in studied

Material	Elastic modulus/GPa	Poisson ratio
Host material	72	0.3
Adhesive	2	0.4
Coating	0.0067	0.49
Optical fiber	72	0.17

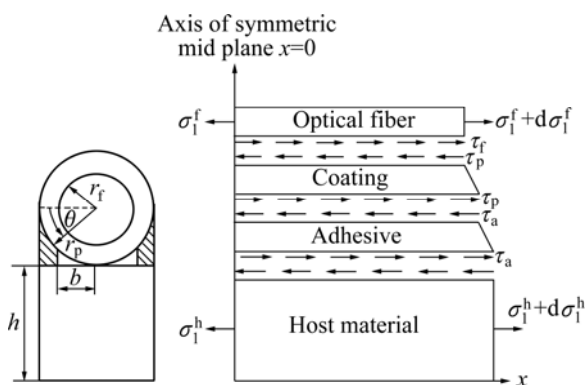


**Fig.1** Analytical model of surface bonded optical fiber

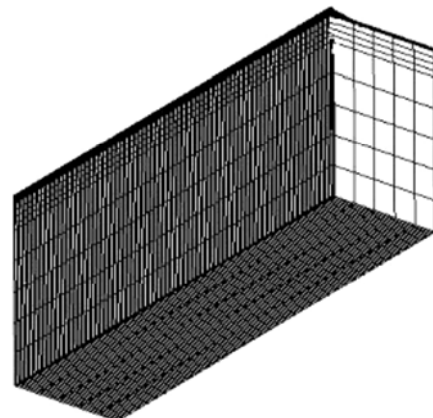


**Fig.2** Finite element mesh

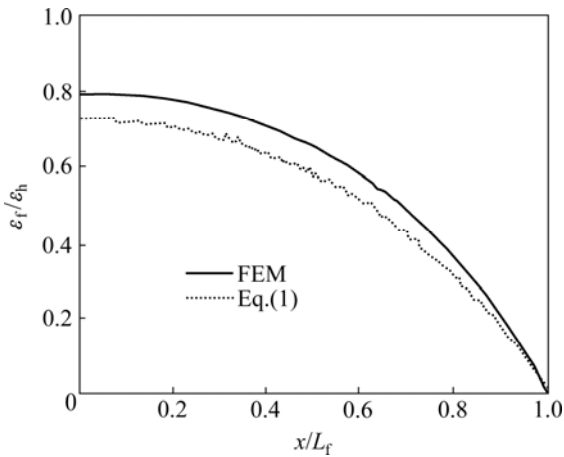


**Fig.3** Normalized strain along optic fiber obtained by FEM and Eq.(1)

**3.1 Influence of surface bonding length**

The variety of surface bonded length,  $2L_f=40, 60, 80, 100, 120$  mm, is proposed to study the influence of the bonded length on the optical fiber strain when the host material is subjected to a far field strain  $\epsilon_0$ . Fig.4 shows the results of normalized optical fiber strain  $\epsilon_f/\epsilon_0$  along the bonded region calculated by Eq.(1) with different bonded length. It is clearly indicated that the longer the bonded length is, the more the strain is transferred to the optic fiber. A steady strain can be achieved in the middle of optical fiber only when the bonded length is long enough. The strain in the optic fiber is less than the far field strain due to the shear deformation at the coating and adhesive.

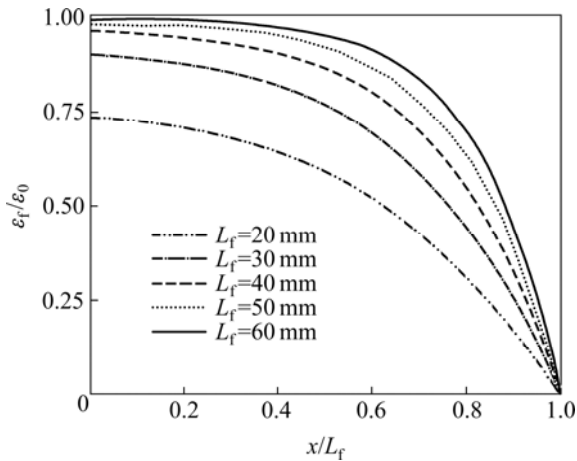


**Fig.4** Normalized strain along optic fiber with different bonded length

**3.2 Influence of elastic modulus of adhesive**

The host material, coating and optic fiber are the same as previous examples listed in Table 1. The elastic modulus of the adhesive is varied from  $0.001E_a$  to  $1\ 000E_a$  ( $E_a=2$  GPa). Fig.5 represents the normalized strain of the optic fiber along the bonded length ( $2L_f=$

40 mm) with different modulus of the adhesive. From this figure, it is apparently demonstrated that the strain transfer increases as the elastic modulus of the adhesive increases. The results indicate that if a high elastic modulus of material is used as the adhesive, the interface bonding becomes more tight. Thus, the strain transferring from the host to the optic fiber becomes more sufficiency.

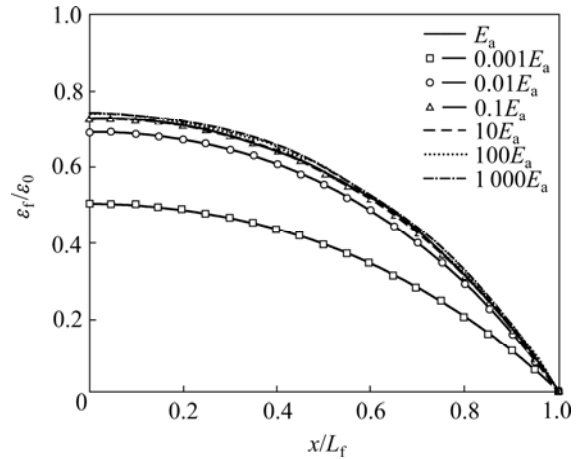


**Fig.5** Normalized strain along optic fiber with different elastic modulus of adhesive

**3.3 Influence of elastic modulus of coating**

The host material, adhesive and optic fiber are the same as previous examples listed in Table 1. The elastic modulus of the coating is varied from  $0.001E_p$  to  $1\ 000E_p$  ( $E_p=6.7$  MPa). Fig.6 shows the normalized strain of the optic fiber along the bonded length ( $2L_f=40$  mm) with different elastic modulus of the coating. Similar to the influence of the adhesive, the strain transferring increases as the elastic modulus of the coating increases. From Fig.5 and Fig.6, we can infer that the coating has more significant influence on the strain transferring from the host material to the optic while comparing to the adhesive.

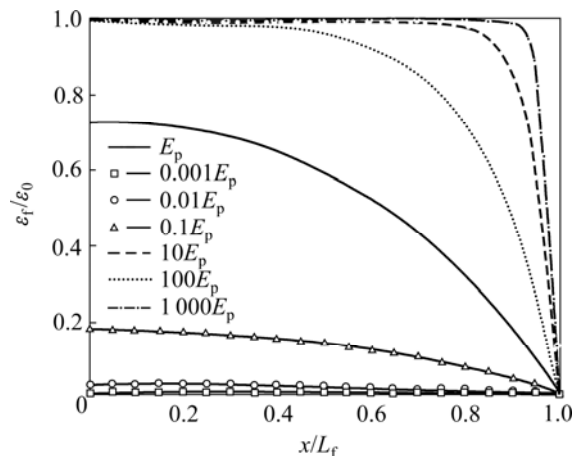


**Fig.6** Normalized strain along optic fiber with different elastic modulus of coating

### 4 Mach-Zehnder interferometric sensor

Mach-Zehnder optical fiber sensor is perhaps the best known because it was developed first. This interferometer acts in the classic sense by optically interfering the light propagating in the reference and sensing fiber. The schematic diagram of a Mach-Zehnder interferometer is shown in Fig.7. It consists of two  $2 \times 2$  couplers at the input and output. The excitation is applied to the sensing fiber, resulting in optical path difference between the reference and sensing fiber. The light intensity of the output of the Mach-Zehnder interferometer can be expressed as [16].

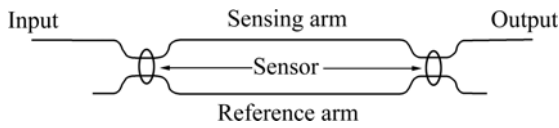


Fig.7 Mach-Zehnder interferometer

$$I = 2A^2(1 + \cos \Delta\phi)$$

$$\Delta\phi = \frac{2\pi n_0}{\lambda} \left\{ 1 - \frac{n_0^2}{2} [(1-\nu)p_{12} - \nu p_{11}] \right\} \int_{\Gamma} \varepsilon_f dx \quad (2)$$

where  $\Delta\phi$  is the optical phase shift;  $n_0$  is the refractive index of the optical fiber;  $\lambda$  is the optical wavelength;  $\nu$  is the Poisson's ratio;  $p_{11}$  and  $p_{12}$  are the Pockel's constants;  $\varepsilon_f$  is the strain of the optical fiber. Since the terms in front of the integral sign of Eq.(2) are constants for any given optical fiber system, the total optical phase shift  $\Delta\phi$  is proportional to the integral of the optical fiber strain. By measuring the total optical phase shift, the integral of the optical fiber strain can be easily obtained as follows:

$$\int_{\Gamma_s} \varepsilon_f dx = \frac{\Delta\phi}{\frac{2\pi n_0}{\lambda} \left\{ 1 - \frac{n_0^2}{2} [(1-\nu_f)p_{12} - \nu_f p_{11}] \right\}} \quad (3)$$

The light intensity shown in Eq.(2) is a cosine function of the optical phase shift  $\Delta\phi$ . Thus, the light intensity of the Mach-Zehnder interferometer exhibits a periodic change with the optical phase shift  $\Delta\phi$ . As the optical phase shift  $\Delta\phi = 2\pi$ , the light intensity goes through a complete cycle. The corresponding integral of the strain is

$$\Delta s = \int_{\Gamma_s} \varepsilon_f dx = \frac{2\pi}{\frac{2\pi n_0}{\lambda} \left\{ 1 - \frac{n_0^2}{2} [(1-\nu_f)p_{12} - \nu_f p_{11}] \right\}} = \frac{\lambda}{n_0 \left\{ 1 - \frac{n_0^2}{2} [(1-\nu_f)p_{12} - \nu_f p_{11}] \right\}} \quad (4)$$

The integral of the strain in Eq.(4) denotes the change of the length of the sensing fiber which is surface bonded on the host material. The average strain of the surface bonded optical fiber for optical phase shift  $\Delta\phi = 2\pi$  is

$$\Delta\varepsilon_{avg} = \frac{\Delta s}{s} = \frac{\int_{\Gamma_s} \varepsilon_f dx}{2L_f} = \frac{\lambda}{2L_f n_0 \left\{ 1 - \frac{n_0^2}{2} [(1-\nu_f)p_{12} - \nu_f p_{11}] \right\}} \quad (5)$$

Eq.(5) represents the average strain of the optical fiber as the light intensity performs one complete cycle. The total average strain of the surface bonded optical fiber can be determined by counting the number of cycles of interferometric light intensity as follows:

$$(\varepsilon_f)_{exp} = \frac{m\lambda}{2L_f n_0 \left\{ 1 - \frac{n_0^2}{2} [(1-\nu_f)p_{12} - \nu_f p_{11}] \right\}} \quad (6)$$

where  $m$  is the number of cycles of light intensity counted from the experimental result, it can be integer or non-integer. Thus, the experimental measurement of the average strain of the surface bonded optical fiber by using the Mach-Zehnder interferometric technique can be obtained from Eq.(6).

The theoretical prediction of the average strain of the surface bonded optical fiber can be deduced from Eq.(1) as

$$(\varepsilon_f)_{the} = \frac{\int_{\Gamma_s} \varepsilon_f(x) dx}{s} = \frac{2 \int_0^{L_f} \frac{\varepsilon_0}{E_f \left( \frac{\pi r_f^2}{2hr_p E_h} + \frac{1}{E_f} \right)} \left[ 1 - \frac{\cosh(\lambda_1 x)}{\cosh(\lambda_1 L_f)} \right] dx}{2L_f} = \frac{\varepsilon_0}{E_f \left( \frac{\pi r_f^2}{2hr_p E_h} + \frac{1}{E_f} \right)} \left[ 1 - \frac{\sinh(\lambda_1 L_f)}{L_f \lambda_1 \cosh(\lambda_1 L_f)} \right] \quad (7)$$

Define the coefficient of strain transformation between the optical fiber and host material as follows:

$$(K)_{exp} = \frac{(\varepsilon_f)_{exp}}{\varepsilon_0} = \frac{m\lambda}{2L_f n_0 \left\{ 1 - \frac{n_0^2}{2} [(1-\nu_f)p_{12} - \nu_f p_{11}] \right\}} \varepsilon_0 \quad (8)$$

$$(K)_{\text{the}} = \frac{(\varepsilon_f)_{\text{the}}}{\varepsilon_0} = \frac{1}{E_f \left( \frac{\pi r_f^2}{2hr_p E_h} + \frac{1}{E_f} \right)} \left[ 1 - \frac{\sinh(\lambda_1 L_f)}{L_f \lambda_1 \cosh(\lambda_1 L_f)} \right] \quad (9)$$

Eq.(8) and Eq.(9) represent the experimental measurement and theoretical calculation of the coefficient of strain transformation, respectively.

### 5 Experimental measurements

A four-point bending test was employed to investigate the strain response measured by the surfaced boned optic fiber sensor. The bending test specimen made of aluminum is shown in Fig.8. A bare optical fiber is bonded on the top surface of the central area of the specimen as the sensing fiber of the Mach-Zehnder interferometer. A strain gauge is bonded on the bottom surface of the specimen to measure the far field strain ( $\varepsilon_0$ ) of the host material induced by the bending test. The material properties of the optical fiber, coating and adhesive are shown in Table 1. The elastic modulus and Poisson’s ratio for the host material (aluminum) are 72 GPa and 0.3, respectively. The wavelength ( $\lambda$ ) of the light emitted from the laser diode to the optic fiber is 1 549.2 nm. The experimental setup is shown in Fig.9. The length of the surface bonded optic fiber is varied from  $2L_f=50$  mm to 120 mm, with the increment of 10 mm in this experimental test. The test specimen is subjected to pure bending.

Fig.10 shows the results of the strain in the specimen measured by the strain gauge and the light intensity of the Mach-Zehnder interferometer with bonded length 50 mm. In the case of bonded length 100 mm, the experimental results are shown in Fig.11. It appears that the number of cycles of the light intensity increases with the increase of the bonded length. Counting the number of cycles of light intensity from Figs.10 and 11 then substituting into Eq.(6) yields to the experimental result of the average strain of the optical fiber. Theoretical prediction of the average strain of the optical fiber is obtained by substituting the strain  $\varepsilon_0$  of the host material measured by the strain gauge into Eq.(7). Table 2 shows the results of the average strain in the optical fiber attained by experimental measurement and theoretical prediction for various bonded length. Good agreement is achieved between the theoretical calculation by Eq.(7) and the experimental measurement by Eq.(6) with the difference less than 8%. Table 3 lists the coefficient of strain transformation between optical

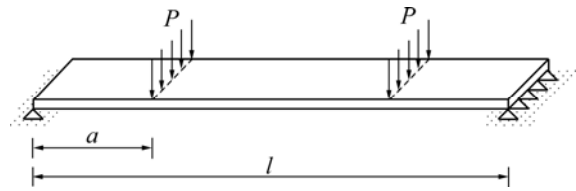


Fig.8 Bending test specimen



Fig.9 Experimental setup of four-point bending measured by Mach-Zehnder interferometry

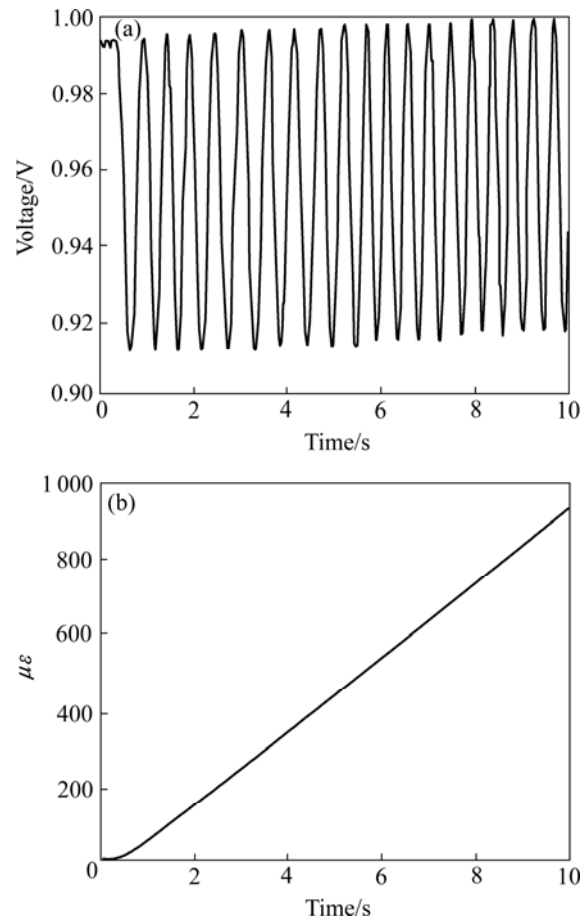
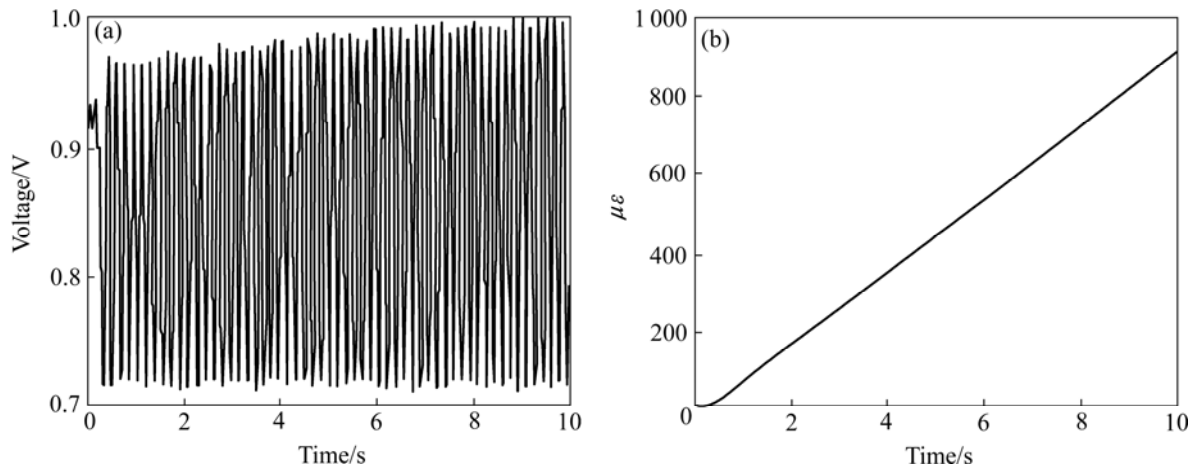


Fig.10 Light intensity of Mach-Zehnder interferometer(a) and strain of host material(b) measured by strain gauge with bonded length 50 mm



**Fig.11** Light intensity of Mach-Zehnder interferometer(a) and strain of host material(b) measured by strain gauge with bonded length 100 mm

**Table 2** Average strain of optic fiber obtained by experimental measurement by Eq.(6) and theoretical calculation by Eq.(7)

Bonded length ( $2L_f$ )/mm	Host material strain $\varepsilon_0$ ( $\mu\varepsilon$ )	Number of cycles	Experimental measurement by Eq.(6) of optic fiber strain $\varepsilon_f$ ( $\mu\varepsilon$ )	Theoretical calculation by Eq.(7) of optic fiber strain $\varepsilon_f$ ( $\mu\varepsilon$ )	Difference/ %
50	891	20	499.29	540.94	7.70
60	931	28	577.88	621.23	7.00
70	901.5	35	622.31	645.72	3.00
80	911.5	47	744.68	688.29	8.19
90	952.5	53	742.14	738.24	1.22
100	950.25	59	742.31	763.24	2.75
110	940.25	66	753.34	768.89	2.02
120	951	74	778.82	788.17	1.18

**Table 3** Strain transformation coefficient ( $K$ ) between optic fiber and host material determined by experimental measurement Eq.(8) and theoretical calculation Eq.(9)

Bonded length( $2L_f$ )/mm	Experimental measurement $K$ by Eq.(8)	Theoretical calculation $K$ by Eq.(9)	Difference/%
50	0.56	0.61	7.4
60	0.62	0.67	6.9
70	0.69	0.72	4.2
80	0.75	0.75	0
90	0.77	0.78	1.6
100	0.78	0.80	2.9
110	0.80	0.82	2.7
120	0.82	0.83	2.3

fiber and host material obtained by experimental measurement Eq.(8) and theoretical calculation Eq.(9). Fig.12 shows the results of the coefficient of strain

transformation varying with the bonded length. From Table 2, Table 3 and Fig.12, the strain of optical fiber is not the same as that of host material. The longer the

bonded length is, the larger the coefficient of strain transformation is, i.e. the more the strain is transferred to the optical fiber.

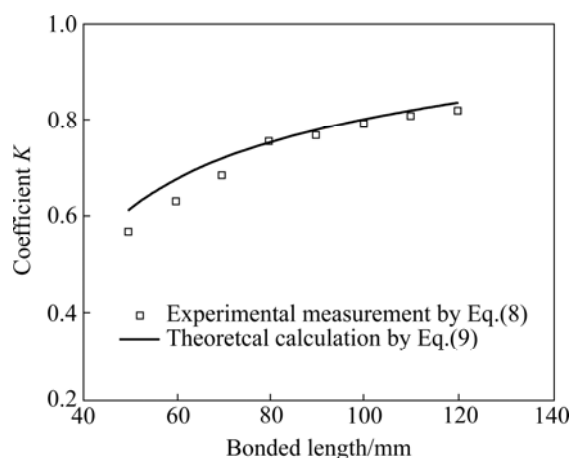


**Fig.12** Coefficient of strain transformation obtained by experimental measurement Eq.(8) and theoretical calculation Eq.(9)

## 6 Conclusions

In this work, the strain of surface bonded optical fiber induced by the host material was presented. Experimental measurement of the optical fiber strain was conducted by using Mach-Zehnder interferometric technique, and compared with the theoretical prediction. Good agreement was observed between experimental measurement and theoretical prediction. The percentage of the strain in the test specimen actually transferred to the optic fiber is dependent on the bonded length of the fiber and material properties of the coating and adhesive. Parametric study shows that the longer the bonded length is and the higher the modulus of the coating is, the more the strain is transferred to the optic fiber.

## Acknowledgement

The authors gratefully acknowledge the financial support under grant No. NSC 93-2212-E-155-007 for this work.

## References

- [1] UDD E. Overview of fiber optic applications to smart structures[C]// Proc 14th Annual Review of Progress in Quantitative Nondestructive Evaluation. New York: Plenum Press, 1988: 541–546.
- [2] ANSARI F. Application of fiber optic sensors in engineering mechanics[C]//ASCE SP. 1993: 1–300.
- [3] MOREY W W. Distributed fiber grating sensors[C]//Proc OFS 90. Sydney, 1990, 285–288.
- [4] MELLE S M, LIU K, MEASURES K. Strain sensing using a fiber optical Bragg grating[J]. SPIE Proc, 1991, 1588: 255–263.
- [5] FOOTE P D. Fiber Bragg grating strain sensors for aerospace smart structures[J]. SPIE Proc, 1994, 2361: 290–293.
- [6] KIM K S, ISMAIL Y, SPRING G S. Measurement of strain and temperature with embedded intrinsic Fabry-Perot optical fiber sensors[J]. J Composite Materials, 1993, 27: 1663–1677.
- [7] HABEL W R, HOFMANN D. Strain measurements in reinforced concrete walls during the hydration reaction by means of embedded fiber interferometers[J]. SPIE Proc, 1994, 2361: 180–183.
- [8] LO Y L. Using in-fiber bragg-grating sensors for measuring axial strain and temperature simultaneously on surfaces of structures[J]. Optical Engineering, 1998, 38: 2276–2282.
- [9] CHAU K, MOSLEHI B, SONG G, SETHI V. Experimental demonstration of fiber bragg grating strain sensors for structural vibration control[J]. SPIE Proc, 2004, 5391: 753–764.
- [10] CRANE R M, GAGORIK J. Fiber optics for a damage assessment system for fiber reinforced plastic composite structure[J]. Quant NDE, 1984, 28: 1419–1430.
- [11] GLOSSOP N D W, DUBOIS S, TSAW W, LEBLANC M, LYMER J, MEASURES R M, TENNYSON R C. Optical fibre damage detection for an aircraft composite leading edge[J]. Composites, 1990, 21: 71–80.
- [12] ELVIN N, LEUNG C K Y, SUDARSHANAM V S, EZEKIEL S. A novel fiber optic delamination detection scheme theoretical and experimental feasibility studies[J]. J Intel Mater Sys Struct, 1999, 10: 314–321.
- [13] XU Y, LEUNG C K Y, YANG Z L, TONG P, LEE S K L. A new fiber optic based method for delamination detection in composites[J]. Struct Health Monitor, 2003, 2: 205–223.
- [14] LAU K T, YUAN L M, ZHOU L, WU J, WOO C H. Strain monitoring in FRP laminates and concrete beams using FBG sensors[J]. Composite Structures, 2001, 51: 9–20.
- [15] HER S C, TSAI C Y. Experimental measurement of fiber-optic strain sensor[J]. SPIE Proc, 2006, 6167: H1–12.
- [16] SIRKIS J S. Unified approach to phase-strain-temperature models for smart structure interferometric optical fiber sensors (Part 1): Development[J]. Optical Engineering, 1993, 32: 752–761.

(Edited by YUAN Sai-qian)